Multi-quasiparticle isomers in ^{174}Lu

F. G. Kondev,[1] G. D. Dracoulis,[2] G. J. Lane,[2] I. Ahmad,[1] A. P. Byrne,[2,3] M. P. Carpenter,[1] P. Chowdhury,[4] R. V. F. Janssens,[1] T. Kibédi,[2] T. Lauritsen,[1] C. J. Lister,[1] D. Seweryniak,[1] S. K. Tandel,[4,*] and S. Zhu[1]

[1]*Argonne National Laboratory, Argonne, Illinois 60439, USA*

[2]*Department of Nuclear Physics, Australian National University, Canberra ACT 0200, Australia*

[3]*Department of Physics, The Faculties, Australian National University, Canberra ACT 0200, Australia*

[4]*Department of Physics, University of Massachusetts Lowell, Lowell, Massachusetts 01854, USA*

(Received 22 November 2008; published 6 July 2009)

Four-, six-, and eight-quasiparticle isomers with $K^\pi = 14^-$, (21^+) and (26^-) have been identified in the deformed nucleus ^{174}Lu, in addition to the previously reported $K^\pi = 13^+$, four-quasiparticle isomeric state. Analysis of alignments and in-band crossover-to-cascade branching ratios lead to the characterization of the configurations associated with the $K^\pi = 14^-$ and (21^+) isomers. The excitation energies of the observed states are compared with results from multi-quasiparticle calculations that include effects of blocking and residual nucleon-nucleon interactions. Good agreement is found for medium-spin ($I = 13$–$14\hbar$) and the highest spin ($I > 20\hbar$) states observed, but there remain ambiguities in assigning configurations in the $I = 15$–$19\hbar$ region.

DOI: 10.1103/PhysRevC.80.014304 PACS number(s): 21.10.Re, 21.10.Tg, 23.20.Lv, 27.70.+q

I. INTRODUCTION

Spectroscopic studies of deformed, axially-symmetric nuclei provide valuable information on properties of high-K isomers that are frequently observed in deformed rare-earth nuclei near $A \sim 180$ [1]. Most of the earlier studies in this region have focused on neutron-deficient nuclei, since these are accessible by heavy-ion induced fusion-evaporation reactions. More recently, deep-inelastic and multinucleon transfer reactions, in conjunction with time correlated γ-ray coincidence techniques and large γ-ray detector arrays, have been shown to be a powerful, although nonselective, tool to access neutron-rich nuclei, as well as to study nuclei near the valley of stability, where most of the long-lived isomers occur [2–10].

Gamma-ray spectroscopy measurements of the deformed nucleus ^{174}Lu have been carried out previously using the ^{170}Er(^{7}Li,3n) [11] and ^{176}Yb(p,3n) [12–16] reactions, where many two-quasiparticle structures, up to spins of $\sim 15\hbar$, were populated. However, the proximity of ^{174}Lu to the stability line limits the possibilities of populating this nucleus to high spin with conventional reactions. In our studies using deep inelastic and multinucleon transfer reactions, much higher spins are accessible, as will be shown here. A report of our identification of a four-quasiparticle, $K^\pi = 13^+$ isomer in ^{174}Lu with anomalous decays was presented recently [9]. Here we give more complete results, focusing on the discovery of four-, six-, and eight-quasiparticle isomers with $K^\pi = 14^-$, (21^+) and (26^-), respectively, all located above the $K^\pi = 13^+$ isomeric state.

[*]Present address: National Nuclear Data Center, Brookhaven National Laboratory, Upton, NY 11973, USA.

II. EXPERIMENTAL DETAILS AND RESULTS

A. Experiments

The results presented here were obtained in measurements with a ^{136}Xe beam from the ATLAS accelerator at Argonne National Laboratory incident on two, $\sim$6 mg/cm^2-thick, Lu targets, one of natural lutetium (97.4% ^{175}Lu, 2.6% ^{176}Lu) and the second enriched to 47% in ^{176}Lu. Both targets were backed by 25 mg/cm^2 of Au. The beam was pulsed approximately 1 ns on/820 ns off at energies $\sim$20% above the Coulomb barrier, which allowed transfers of nucleons between the target and projectile. This resulted in population of nuclei near the valley of stability, or on the neutron-rich side, that were not accessible previously. The reaction products were stopped at the target position in the focus of the Gammasphere spectrometer [17], comprised for this experiment of 96 Compton-suppressed Ge detectors. A total of approximately 3×10^9 events, with fold $\geqslant 3$, was collected. The data were sorted off line into numerous γ-γ and γ-γ-γ histograms produced with different relative and absolute time (with respect to the beam pulse) and energy gating conditions, as described in Refs. [5–9].

B. ^{174}Lu level scheme

A level scheme of ^{174}Lu from the present study, showing the decay paths of the newly identified isomers, is presented in Fig. 1.

Details about the properties of the strongly populated $K^\pi = 13^+$ isomer at 1856 keV were discussed earlier [9]. Several representative γ-ray coincidence spectra showing γ rays above this isomer are given in Fig. 2. Various relative and absolute time conditions were imposed to select specific structures.

For example, Fig. 2(a) is the spectrum of γ rays that precede the decay of the 13^+ isomer and also fall within the in-beam time region. These will either be from states that are prompt

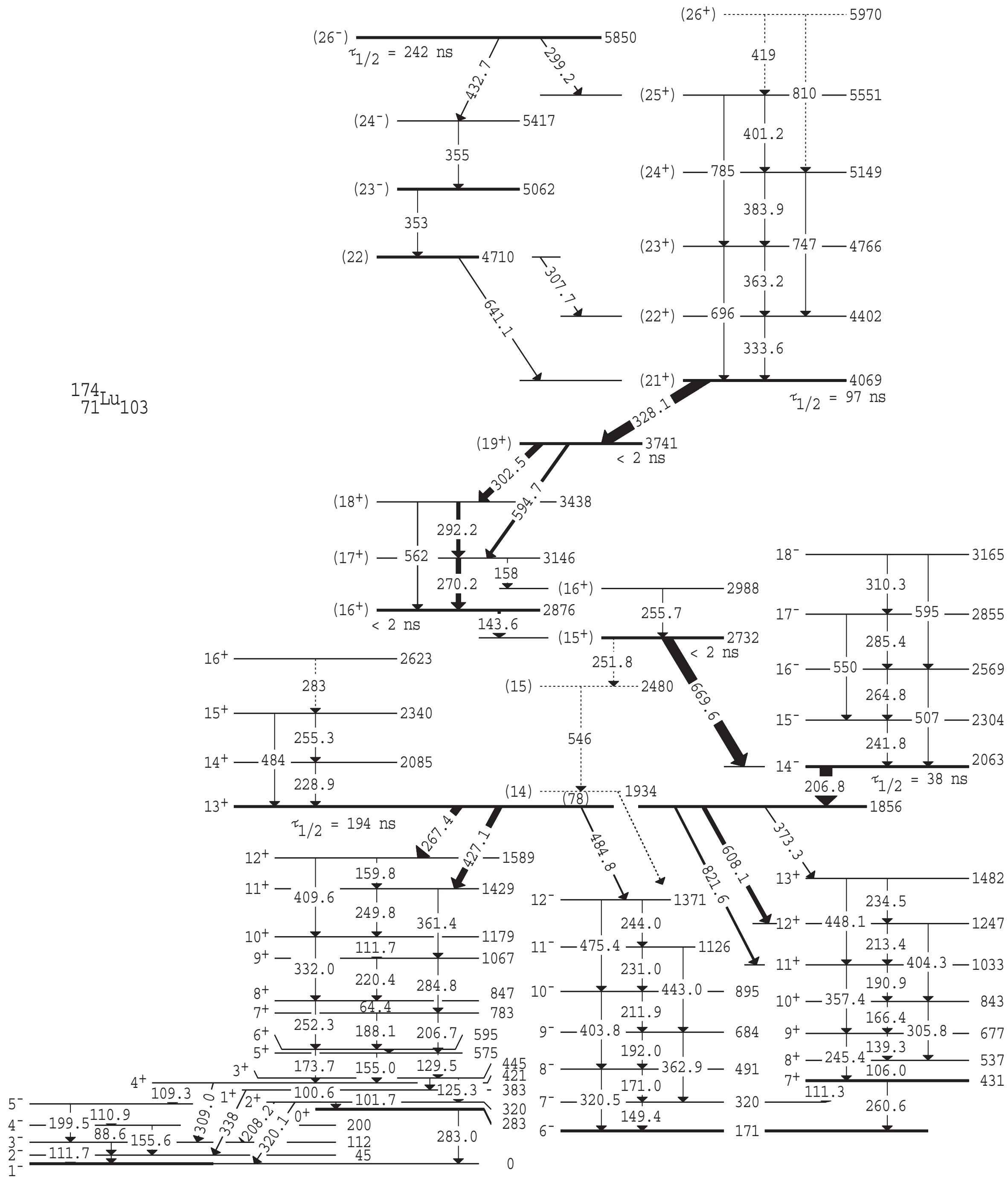

FIG. 1. Partial level scheme of ^{174}Lu showing the decay of the $K^{\pi} = 13^{+}$ isomer [9] and structures located above it. Note that for clarity, not all transitions associated with the low-lying $K^{\pi} = 0^{+}$ and 1^{-} bands are given. Transition energies are accurate to within ±0.3 keV.

or originate from short isomers, hence the presence of the intense 206.8-keV line from the 2063-keV, 38 ns isomer that directly feeds the 13^{+} state. The next most intense line is that at 669.6 keV, placed as a direct feed to the 2063-keV state. The spectrum in Fig. 2(b) is constructed using γ-ray energy and relative time gates selecting transitions above the 13^{+} isomer, but with the additional condition that they occur in the out-of-beam time region. Hence, these γ rays must be fed by higher-lying isomers. The spectrum shown in the lowest panel, Fig. 2(c), is produced by gating on the delayed γ rays that are in cascade below the 4069-keV level, selecting transitions that feed it and are also out-of beam. The transitions in this spectrum are largely from the main branch (299.2 keV) of the uppermost isomer and the cascade and crossover transitions in the band based on the 4069-keV isomeric state.

The ordering of the main transitions between the 4069-keV isomeric state and the 2063-keV isomer, particularly the 328.1- and 669.6-keV γ rays, is evident from the delayed/prompt

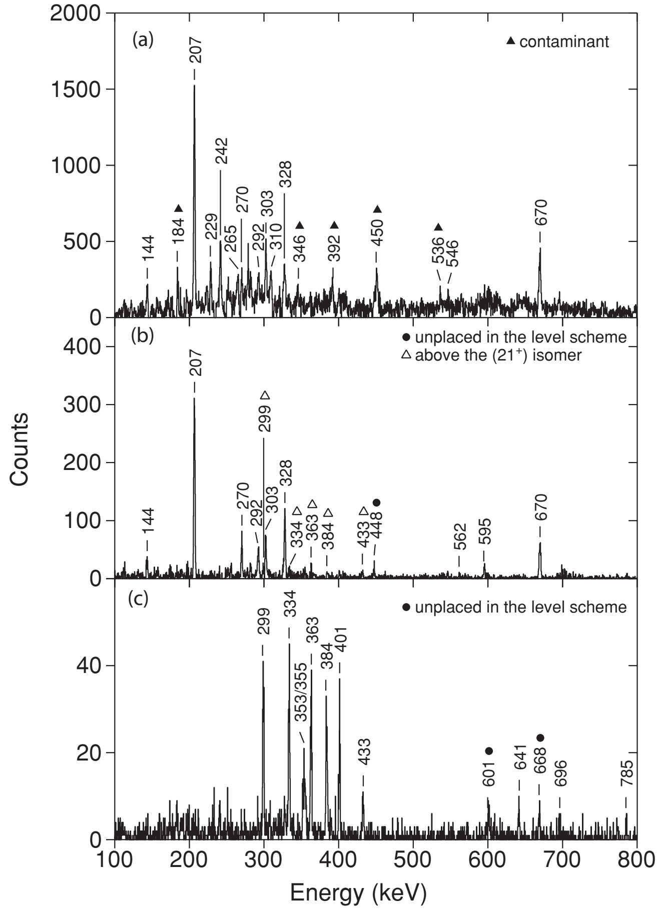

FIG. 2. (a) "Early" spectrum showing γ rays above the $K^{\pi} = 13^{+}$ isomer [9] in the in-beam time region. The spectrum was produced by summing "delayed" gates (in the interval 30 to 770 ns after the beam pulse) on the 260.6- and 267.4-keV γ rays below the 13^{+} isomer; (b) same as (a), but requiring the γ rays to fall between beam pulses; (c) "Early" spectrum showing γ rays located above the $K^{\pi} = (21^{+})$ isomer at 4069 keV in the out-of-beam time region (see text).

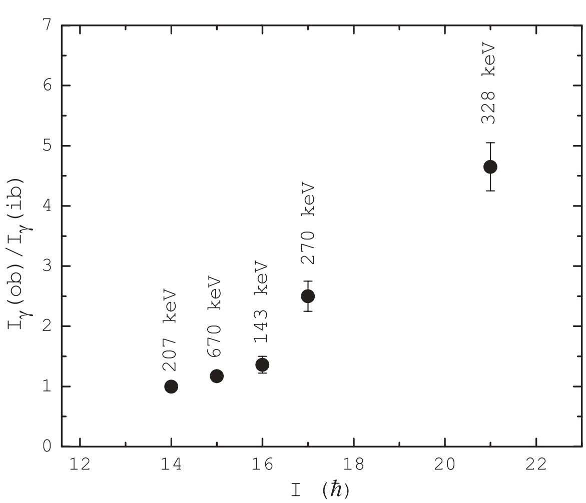

FIG. 3. Out-of-beam (ob) to in-beam (ib) intensity ratios for selected transitions above the $K^{\pi} = 13^{+}$ isomer. The data are normalized to a ratio of unity for the 207-keV γ ray.

intensity ratios deduced from the spectra of Figs. 2(a) and 2(b). The ratios given in Fig. 3, for example, indicate that the 669.6-keV transition has significant prompt side-feeding, consistent with it originating from a lower-spin state and not directly from an isomer.

The $K^{\pi} = 14^{-}$ assignment to the 2063-keV isomer follows from the $E1$ character of the 206.8-keV depopulating transition. The total conversion coefficient $\alpha_T^{\rm exp}(206.8) < 0.2$, extracted from intensity balances, can be compared with theoretical values of 0.05, 0.47, and 0.25 for $E1$, $M1$, and $E2$ multipolarities, respectively [18]. The spin and parity assignments to the other two isomers are less certain, as they are based mainly on their decay patterns.

The main intensity below the $K^{\pi} = (16^{+})$ state at 2876 keV is carried by the 143.6-669.6-206.8 keV sequence. The 143.6-keV transition is highly converted with $\alpha_T^{\rm exp} = 1.1(2)$, to be compared with theoretical values of 0.14 ($E1$), 1.3 ($M1$), and 0.87 ($E2$) [18], suggesting a $M1$ multipolarity, with possibly a small $E2$ admixture. This transition is assigned as a connection between two intrinsic states at 2876 and 2732 keV, neither of which has a significant half-life. The 255.7-keV transition feeding the 2732-keV state is probably the first transition in the rotational band built on the top of this level. Two members of the band based on the 2876-keV $K^{\pi} = (16^{+})$ state are identified, as shown in Fig. 1 with both cascade and crossover transitions observed. While the level at 3741 keV exhibits decays which could identify it as the next member of the band, the transition energies are about 10 keV lower than expected, thus it is proposed to correspond to another intrinsic state.

The 3741-keV state decays via the 302.5-keV (dipole) and 594.7-keV (quadrupole) transitions to the (18^{+}) and (17^{+}) members of the $K^{\pi} = (16^{+})$ band with a branching ratio of $I_{\gamma}(594.7)/I_{\gamma}(302.5\ \text{keV}) = 0.47(5)$, which is similar to that expected for an in-band state. This could be taken as an indication that there has been mixing between the intrinsic state and the (unobserved) 19^{+} member of the band (as discussed in Refs. [6,9]). (Note that if the depopulating transitions were both of dipole character, one would expect $I_{\gamma}(594.7\ \text{keV})/I_{\gamma}(302.5\ \text{keV}) \approx (595/303)^3 = 7.6$.)

The 3741-keV (19^{+}) state is directly fed via the 328.1-keV transition from the 4069-keV isomer. In the out-of-beam γ-γ coincidence data there are several other weak γ rays (e.g., at 173.8, 188.1, 219.2, and 260.4 keV) that are apparently in coincidence with the 270.2-, 302.5-, and 328.1-keV transitions in this part of the scheme. However, because of their low intensity, we were unable to either assign them unambiguously to ^{174}Lu or to place them in the level scheme. The situation is complicated further by self-coincidence relationships, which indicate the presence of at least two 546-keV transitions. The latter coincide as well in energy with the 547.5-keV ^{197}Au line from the target backing that is strong in the in-beam period.

The rotational band above the (21^{+}) state is identified through coincidences which extend into the prompt beam-pulse as well as into the out-of-beam regions due to feeding from the 5850-keV, 242-ns isomer [Fig. 2(c)]. The latter isomer, with a proposed $K^{\pi} = (26^{-})$ assignment, decays into the (25^{+}) level of the $K^{\pi} = (21^{+})$ band (~78% via the 299.2-keV transition) and also through a parallel path. On the basis of energies, the 5417-keV state is a candidate for the first

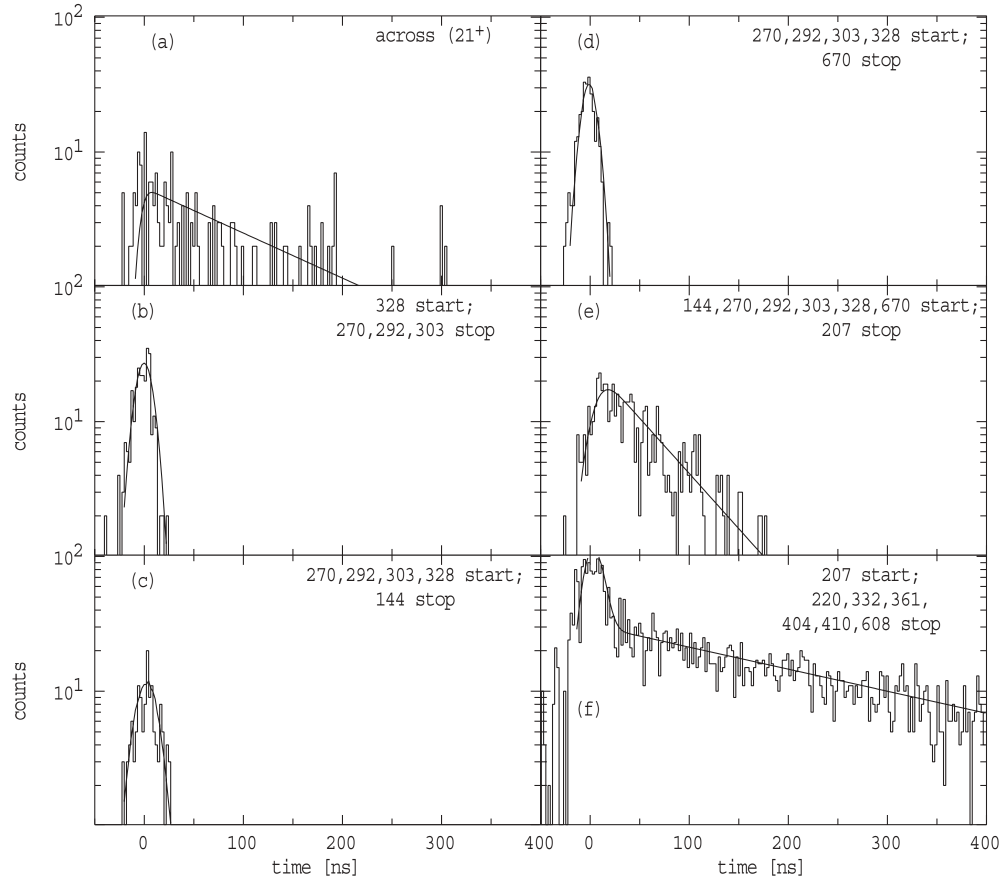

FIG. 4. Time-difference spectra for selected levels in ^{174}Lu produced by gating on γ rays above and below the level of interest, as indicated.

member of a band based on the 5062-keV state, but otherwise there is minimal information on which to define the character of the states in this sequence, the 4710- and 5062-keV levels possibly being intrinsic states.

It was also not possible to identify any transitions feeding the uppermost isomer, despite the fact that the half-life is ideal for using early-delayed coincidence relationships to isolate transitions above it. This is not surprising since the spin population in these reactions drops rapidly in the spin region above $20\hbar$.

C. Lifetimes

The lifetimes of the isomeric states were deduced from a variety of sources including timing with respect to the pulsed beam, as well as projections of intermediate time spectra in cases where there was sufficient intensity to gate on transitions directly above and below the level of interest. Examples are shown in Figs. 4 and 5.

Figure 4 gives intermediate time spectra from the time-γ-γ data for selected cases. Figure 4(a) for example, was produced by gating on a number of transitions above and below the 4069-keV state, only using the out-of-beam time region. The statistics in this case are low because these constraints select only the population that proceeds through the highest (weakly populated) isomer. The superimposed curve in Fig. 4(a) is a fit to the intensity, but with a half-life fixed at the value deduced from the curve for the (21^+) isomer, shown in Fig. 5. Figures 4(b), 4(c), and 4(d) indicate that the 3741-, 2876-, and 2732-keV states do not have significant lifetimes, leading

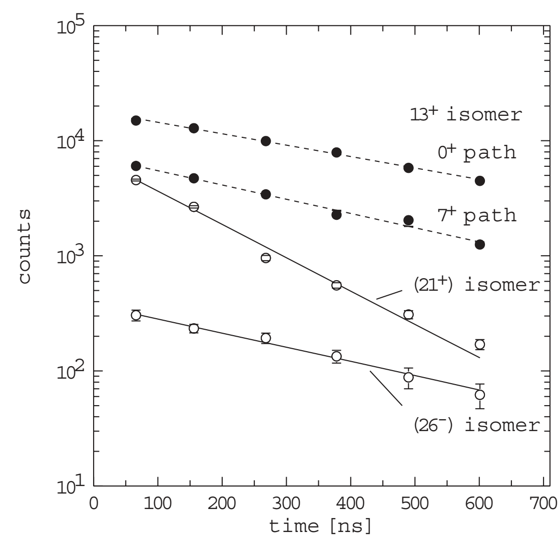

FIG. 5. Decay curves for isomers in ^{174}Lu obtained from the intensities of γ rays in double-gated spectra produced from γ-γ-γ cubes in six sequential out-of-beam time regions.

TABLE I. Half-lives and transition probabilities in ^{174}Lu.

E_γ (keV)	Mult.	I_γ[a] (rel)	α_T[b]	$1/F$[c] W.u.	ν[d]	f_ν[e]
$K^\pi = 13^+$	$E = 1856$ keV	$T_{1/2} = 194$ (24) ns				
267.4	$M1$	100 (5)	0.233	$1.9\ (3) \times 10^{-6}$	12	2.99 (4)
373.3	$M1$	7.7 (16)	0.0954	$5.5\ (14) \times 10^{-8}$	5	28.3 (14)
427.1	$E2$	80.8 (42)	0.0280	$9.4\ (13) \times 10^{-4}$	11	1.885 (24)
484.8	$E1$	15.6 (20)	0.00675	$5.0\ (9) \times 10^{-10}$	6	35.5 (11)
608.1	$M1$	50 (4)	0.0268	$8.2\ (13) \times 10^{-8}$	5	26.1 (8)
821.6	$E2$	25 (3)	0.00568	$1.10\ (20) \times 10^{-5}$	4	17.4 (8)
$K^\pi = 14^-$	$E = 2063$ keV	$T_{1/2} = 38(4)$ ns				
206.8	$E1$	100	0.0525	$6.1\ (7) \times 10^{-7}$		
$K^\pi = (15^+)$	$E = 2732$ keV	$T_{1/2} < 2$ ns				
669.6	$E1$	100	0.0034	$>3.5 \times 10^{-7}$		
$K^\pi = (16^+)$	$E = 2876$ keV	$T_{1/2} < 2$ ns				
143.6	$E1$	100	1.311	$>1.5 \times 10^{-3}$		
$K^\pi = (19^+)$	$E = 3741$ keV	$T_{1/2} < 2$ ns				
302.5	$M1$	100 (5)	0.167	$>2.3 \times 10^{-4}$	2	<66
594.7	$E2$	47 (5)	0.012	$>1.8 \times 10^{-2}$	2	<55
$K^\pi = (21^+)$	$E = 4069$ keV	$T_{1/2} = 97$ (10) ns				
328.1	$E2$	100	0.0587	$2.5\ (3) \times 10^{-2}$		
$K^\pi = (26^-)$	$E = 5850$ keV	$T_{1/2} = 242$ (19) ns				
299.2	$E1$	100 (9)	0.0208	$2.6\ (4) \times 10^{-8}$	4	79 (3)
432.7	$E2$	28 (5)	0.0270	$5.7\ (12) \times 10^{-4}$	1	1700 (400)

[a]Relative gamma-ray intensity. The strongest transition that depopulates a particular level is assumed to have $I_\gamma = 100$.
[b]Total electron conversion coefficient from Ref. [18].
[c]Hindrance factor, $F = T^{\gamma}_{1/2}/T^{W}_{1/2}$, where $T^{\gamma}_{1/2}$ and $T^{W}_{1/2}$ are the partial γ-ray and the Weisskopf estimate half-lives, respectively.
[d]Degree of K-forbiddenness, $\nu = \Delta K - \lambda$, where λ is the transition multipolarity.
[e]Reduced hindrance factor per degree of K-forbiddenness, $f_\nu = F^{1/\nu}$.

essentially to a limit of $T_{1/2} < 2$ ns for each of these levels. These values were deduced using a centroid-shift method, which is similar to that reported in Ref. [19]. Figure 4(e) provides the intermediate time spectrum for the 2063-keV state, while Fig. 4(f) gives the time spectrum obtained by gating above and below the 13^+ isomer. (The small prompt component in this spectrum is due to contaminants present in some of the gates.)

The decay curves in Fig. 5 were produced by constructing γ-γ-γ cubes with gates on six contiguous out-of-beam time regions. A combination of double gates in the path below each isomer was applied to these cubes to produce spectra from which time-dependent intensities were extracted. In principle, these curves will be complex because of the presence of more than one feeding path, but the rapid fall in population with spin means that this effect is of relatively minor significance, although it was included in the analysis. It should be emphasized that the half-lives were deduced from several complementary sources, as discussed above. The final values are presented in Table I, together with the derived transition strengths.

III. MULTI-QUASIPARTICLE CALCULATIONS AND CONFIGURATIONS

Predictions of the excitation energy, spin and parity for states in ^{174}Lu were obtained using multi-quasiparticle blocking calculations, similar to those reported elsewhere (see for example Refs. [6,7] and references therein). Specifically, the set of single-particle orbitals originating from the $N = 4, 5$, and 6 (neutrons) and 3, 4, and 5 (protons) oscillator shells were taken from the Nilsson model with parameters κ and μ from Ref. [20], and deformations $\varepsilon_2 = 0.258$ and $\varepsilon_4 = 0.067$ [21]. The states close to the proton and neutron Fermi surfaces were adjusted to reproduce approximately the experimental one-quasiparticle average energies in ^{173}Lu and ^{175}Lu (for the protons) and ^{175}Hf (for the neutrons) [22,23]. The latter choice, rather than an average of ^{173}Hf and ^{175}Hf, is adopted because the deformation in ^{174}Lu is predicted to be closer to that of ^{175}Hf. The pairing correlations were treated using the Lipkin-Nogami prescription with fixed strengths of $G_\pi = 20.8/A$ MeV and $G_\nu = 18.0/A$ MeV. The predicted energies of the multi-quasiparticle states were subsequently corrected for the effect of residual interactions using the prescription of Ref. [24] and the energies associated with the Gallagher-Moszkowski splitting of Ref. [25], except for the $\nu(5/2^-[512]) \otimes \pi(7/2^-[523])$ configuration for which the value recently reported in Ref. [26] was used. The calculated excitation energies for yrast and near-yrast high-K states in ^{174}Lu, together with the experimental observations, are summarized in Table II.

A. $K^\pi = 13^+$ isomer at 1856 keV

The $K^\pi = 13^+$ isomer decays to the $K^\pi = 0^+, 7^+$, and 6^- two-quasiparticle bands and was assigned the $\nu^3(5/2^-[512],$

TABLE II. Calculated and experimental states in ^{174}Lu.

K^π	Configuration[a]		$E_{\rm qp}$[b]	$E_{\rm res}$[c]	$E_{\rm calc}$[d]	$E_{\rm expt.}$[e]
	ν	π	(keV)			
1^-	5/2-	$7/2^+$	0	−56	**0**	**0**
6^-	$5/2^-$	$7/2^+$	0	56	112	171
0^+	$7/2^+$	$7/2^+$	211	−63	204	281
7^+	$7/2^+$	$7/2^+$	211	+63	330	431
13^+	$5/2^-,7/2^-,7/2^+$	$7/2^+$	1777	−37	1796	1856
14^-	$5/2^-,7/2^+,9/2^+$	$7/2^+$	1998	+760	2814	
14^-	$5/2^-,7/2^-,7/2^+$	$9/2^-$	2209	−133	2132	2063
15^+	$7/2^+$	$7/2^+,7/2^-,9/2^-$	2657	−190	2523	
15^+	$5/2^-,7/2^+,9/2^+$	$9/2^-$	2429	+351	2836	(2732)
15^-	$7/2^-,7/2^+,9/2^+$	$7/2^+$	2637	+14	2707	
16^+	$9/2^+$	$7/2^+,7/2^-,9/2^-$	3085	−215	2926	
16^+	$7/2^-,7/2^+,9/2^+$	$9/2^-$	3068	−78	3046	(2876)
19^-	$5/2^-,7/2^-,7/2^+$	$5/2^+,7/2^+,7/2^-$	4151	−371	3836	
19^+	$1/2^-,5/2^-,7/2^-,7/2^+,9/2^+$	$9/2^-$	4036	−174	3918	(3741)
21^+	$5/2^-,7/2^-,7/2^+$	$7/2^+,7/2^-,9/2^-$	4223	−373	3906	4069
22^-	$5/2^-,7/2^+,9/2^+$	$7/2^+,7/2^-,9/2^-$	4444	+190	4690	(4710)*
22^+	$5/2^-,7/2^-,9/2^+$	$7/2^+,7/2^-,9/2^-$	5043	−407	4692	(4710)*
23^-	$7/2^-,7/2^+,9/2^+$	$7/2^+,7/2^-,9/2^-$	5083	−289	4850	(5062)
26^-	$1/2^-,5/2^-,7/2^-,7/2^+,9/2^+$	$7/2^+,7/2^-,9/2^-$	6050	−374	5732	5850

[a]**Neutrons** (ν): $1/2^-$: $1/2^-[521]$; $5/2^-$: $5/2^-[512]$; $7/2^-$:$7/2^-[514]$; $7/2^+$:$7/2^+[633]$; $9/2^+$:$9/2^+[624]$. **Protons** (π): $5/2^+$:$5/2^+[402]$; $7/2^+$:$7/2^+[404]$; $7/2^-$:$7/2^-[523]$; $9/2^-$:$9/2^-[514]$.
[b]Energies from the multi-quasiparticle calculations.
[c]Residual interactions.
[d]$E_{\rm calc} = E_{qp} + E_{\rm res} + 56$ keV. The addition of the 56 keV term comes from fixing $E_{\rm calc}$ (g.s.) = 0.0 keV.
[e]Experimental energies for the four-, six-, and eight-quasiparticle states are from the present work; two-quasiparticle states are from Refs. [11,12].

$7/2^-[514]$, $7/2^+[633]) \otimes \pi(7/2^+[404])$ configuration in Ref. [9]. The crossover-to-cascade branching ratio, λ, for the $I^\pi = 15^+$ level in the rotational band based on the isomer was used to deduce the intrinsic g factor values, g_K, using conventional rotational model formulas:

$$\frac{g_K - g_R}{Q_0} = 0.933\frac{E_\gamma(I \to I-1)}{(\sqrt{I^2-1})\delta}, \qquad (1)$$

where E_γ is in units of MeV and the mixing ratios, δ, is deduced as

$$\frac{1}{\delta^2} = \frac{1}{\lambda}\left(\frac{E_\gamma(I \to I-2)}{E_\gamma(I \to I-1)}\right)^5 \frac{\langle IK20|I-2K\rangle^2}{\langle IK20|I-1K\rangle^2} - 1. \qquad (2)$$

The quadrupole moment of $Q_0 = 7.65(9)$ eb (the average value for the measured $\pi 7/2^+[404]$ ground state in ^{173}Lu [22] and ^{175}Lu [23]) and the rotational g factor of $g_R = +0.3$ were used. The value of $g_K = 0.40(2)$ was obtained (see Table III) in agreement with the expected value of $g_K = 0.41$, deduced from calculations with Woods-Saxon wave functions for this configuration [27]. (An empirical value of 0.08 has been assumed for the $7/2^+[633]$ ($i_{13/2}$) component [29] to account for Coriolis mixing effects.) The higher alignment of the band associated with the isomer compared to those of the $K^\pi = 6^-$, $\nu(5/2^-[512]) \otimes \pi(7/2^+[404])$ and $K^\pi = 7^+$, $\nu(7/2^+[633]) \otimes \pi(7/2^+[404])$ bands, shown in Fig. 6, supports the presence of a single $i_{13/2}$ neutron in the configuration. There is also good agreement between the energies of the observed and calculated 13^+ states, as presented in Table II.

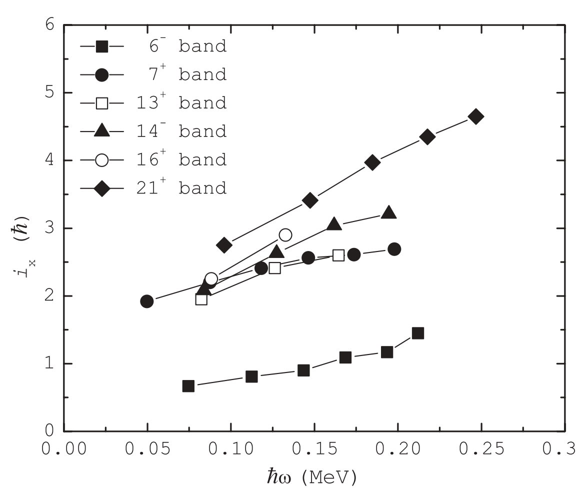

FIG. 6. Alignments for observed bands in ^{174}Lu. Common Harris reference parameters of $\Im_0 = 39$ MeV$^{-1}\hbar^2$ and $\Im_1 = 70$ MeV$^{-3}\hbar^4$ were used for all bands.

TABLE III. Branching ratios and g_K-g_R values for states within the $K^\pi = 13^+$, 14^-, (16^+) and (21^+) bands in ^{174}Lu.

I^π	$E_\gamma(\Delta I = 1)$ (keV)	$E_\gamma(\Delta I = 2)$ (keV)	λ[a]	$\lvert g_K\text{-}g_R\rvert$[b]
$K^\pi = 13^+$				
15^+	255.3	484	0.66(8)	0.097(18)
$K^\pi = 14^-$				
16^-	264.8	507	0.65(8)	0.091(17)
17^-	285.4	550	1.49(25)	0.085(22)
$K^\pi = 16^+$				
18^+	292.2	562	0.21(5)	0.217(4)
$K^\pi = 21^+$				
23^+	363.2	696	0.10(3)	0.268(8)
24^+	383.9	747	0.13(4)	0.370(10)
25^+	401.2	785	0.28(6)	0.312(5)

[a]Crossover-to-cascade branching ratios, $\lambda = I_\gamma(I \to I-2)/I_\gamma(I \to I-1)$.
[b]Deduced using the measured crossover-to-cascade branching ratios (λ) and the standard rotational model formulas [see Eqs. (1) and (2)] with $Q_0 = 7.65$ (9) eb.

B. $K^\pi = 14^-$ isomer at 2063 keV

The $K^\pi = 14^-$ isomer can be associated with the predicted $\nu^3(5/2^-[512],7/2^-[514],7/2^+[633]) \otimes \pi(9/2^-[514])$ configuration. The value of $g_K = 0.39(2)$, weighted average of these deduced for levels up to $I^\pi = 17^-$ in the rotational band based on the isomer, was obtained (see Table III). It agrees well with the expected value of $g_K = 0.44$, deduced from calculations with Woods-Saxon wave functions for this configuration [27]. It should be noted that a value of $g_K = 0.12$ could be expected for the alternative $\nu^3(5/2^-[512],7/2^+[633],9/2^+[624]) \otimes \pi(7/2^+[404])$ configuration that is predicted at higher excitation energy (see Table II). The observed alignment for the $K^\pi = 14^-$ band (Fig. 6) supports the presence of a single $i_{13/2}$ neutron in the configuration of this structure. In addition, the configuration is related to that of the $K^\pi = 13^+$ isomer with the $7/2^+[404]$ proton orbital replaced by the $9/2^-[514]$ one. The deduced transition strength of 5.4 (12) $\times 10^{-7}$ W.u. for the depopulating 206.8 keV $E1$ transition is in good agreement with those of 6.6 (2) $\times 10^{-7}$ W.u., 3.64 (14) $\times 10^{-7}$ W.u., and 7.3 (4) $\times 10^{-7}$ W.u. observed for the $\pi 9/2^-[514] \to \pi 7/2^+[404]$ transition in the neighboring ^{175}Lu, ^{175}Ta and ^{177}Ta nuclei, respectively [23,30].

C. $K^\pi = (21^+)$ isomer at 4069 keV

Calculations predict a $K^\pi = 21^+$, six-quasiparticle state arising from the

$$\nu^3(5/2^-[512], 7/2^-[514], 7/2^+[633]) \otimes \pi^3(7/2^+[404], 7/2^-[523], 9/2^-[514])$$

configuration at 3906 keV. This state can presumably be associated with the isomer at 4069 keV. The deduced value of $g_K = 0.61(1)$ from the in-band branching ratios agrees well with that of 0.62 expected from calculations with Woods-Saxon wave functions [27] for this configuration. Although both the $K^\pi = 21^+$ and 14^- configurations contain a single $i_{13/2}$ neutron, the alignment of the former is $\sim 0.6\hbar$ higher, due to the presence of an additional high-j, $7/2^-[523]$ ($h_{11/2}$) proton in the proposed configuration.

D. States between the $K^\pi = 14^-$ and (21^+) isomers

The calculations predict two $K^\pi = 15^+$ and two $K^\pi = 16^+$ states in this energy region (see Table II). It should be noted, however, that the configurations of the 15^+ and 16^+ states, predicted at 2523 and 2926 keV, are both $\nu\pi^3$ and are very closely related through substitution of a $9/2^+[624]$ neutron for the $7/2^+[633]$ one. Since both of these orbitals originate from the same $i_{13/2}$ parent, they will be mixed. Experimentally it is seen that the 17^+ state of the $K^\pi = 16^+$ band has a 158-keV γ-ray branch to the 16^+ level of the $K^\pi = 15^+$ band, in competition with the in-band cascade, consistent with mixing. However, the $15^+/16^+$ pair from $\nu^3\pi$ configurations predicted at 2836 and 3046 keV are also closely related, with an exchange of only a $5/2^-[512]$ neutron for a $7/2^-[514]$ one. The deduced g_K value of 0.52(1) for the $K^\pi = 16^+$ band based on the 2876-keV state is, in fact, in agreement with the predicted value of 0.47 for the $\nu^3(7/2^-[514], 7/2^+[633],9/2^+[624]) \otimes \pi(9/2^-[514])$ configuration and significantly smaller than the value of $g_K = 0.80$ expected for the alternative $\nu(9/2^+[624]) \otimes \pi^3(7/2^+[404],7/2^-[523],9/2^-[514])$ configuration that is calculated to be lower in energy. The $\nu^3\pi$ configuration also contains two $i_{13/2}$ neutrons and this should result in a somewhat higher alignment compared to that for the $K^\pi = 14^-$ band, for example. This is indeed seen in Fig. 6, albeit the difference is not as significant as one may expect, which could be indicative that the alternative $\nu\pi^3$ configuration is associated with the $K^\pi = 16^+$ band. Note that, as discussed in Ref. [28], the alignment will not necessarily be additive because there will be configuration-dependent proton and neutron pairing reductions with increasing seniority.

As indicated earlier, the (19^+) level at 3741 keV is interpreted as an intrinsic state, rather than as a rotational band member. It can identified with the predicted 19^+ state associated with the

$$\nu^5(1/2^-[521], 5/2^-[512], 7/2^-[514], 7/2^+[633], 9/2^+[624]) \otimes \pi(9/2^-[514])$$

configuration. The predicted energy for this state is $\sim$170 keV higher than that observed, which may be problematic, given that most other cases are slightly underpredicted. This configuration is unusual in that it has five neutrons and only one proton, which might point to an uncertainty in the energy of the neutron component. However, that component is also common to the 26^- configuration whose energy is reasonably well reproduced.

Note that an assignment of the 3741-keV level as an intrinsic state with $K = 19$ rather than as a $K = 16$ rotational state provides a natural explanation for the relatively fast decay from the $K^\pi = (21^+)$ isomer above, being in this case, only once K-forbidden, as will be discussed below. Also, while the multi-quasiparticle calculations also predict a 19^- state in this region, the lifetime limit is sufficient to exclude the 594.7 keV $M2$ branch that would be implied in such a case.

The lack of a significant lifetime for the $K^\pi = (16^+)$ state at 2876 keV, as evident from Fig. 4(c), could be taken to imply that the (15^+) state at 2732 keV arises from the $\nu^3(5/2^-[512],7/2^+[633],9/2^+[624]) \otimes \pi(9/2^-[514])$ configuration rather than from the $\nu(7/2^+[633]) \otimes \pi^3(7/2^+[404], 7/2^-[523],9/2^-[514])$ alternative. The latter would require a rearrangement of several orbitals between the $K^\pi = (16^+)$ and (15^+) states, and perhaps result in a slower transition. However, this is not a strong argument since the 143.6-keV transition is not K-forbidden and the limit on the half-life ($T_{1/2} < 2$ ns) corresponds to a relatively low transition strength of $>1.5 \times 10^{-3}$ W.u.. The present half-life limit is, therefore, not a significant constraint. Similarly, as will be discussed in the following section, the absence of a significant lifetime for the (15^+) level at 2732 keV [see Fig. 4(d)] is consistent with the proposed $\nu^3\pi$ configurations for both the initial and final states, the implied $E1$ strength for the 669.6-keV transition being low and similar to (normal) $E1$ strengths.

E. $K^\pi = (26^-)$ isomer at 5850 keV

Calculations predict a particularly energy-favored, eight-quasiparticle state at 5732 keV with $K^\pi = 26^-$ from the

$$\nu^5(1/2^-[521], 5/2^-[512], 7/2^-[514], 7/2^+[633], 9/2^+[624]) \otimes \pi^3(7/2^+[404], 7/2^-[523], 9/2^-[514])$$

configuration. We associate this predicted state with the observed uppermost isomer at 5850 keV. Further characterization of this state would require identification of the associated rotational band.

F. Intrinsic states between the $K^\pi = (21^+)$ and (26^-) isomers

The structure of nonrotational states between the $K^\pi = (26^-)$ and (21^+) isomers is less certain. As can be seen from Table II, there are two calculated, nearly degenerate six-quasiparticle states with $K^\pi = 22^-$ and $K^\pi = 22^+$ that are potential candidates for the observed state at 4710 keV. Based on the predicted multi-quasiparticle states, the level at 5062 keV can be associated with the $K^\pi = 23^-$

$$\nu^3(7/2^-[514], 7/2^+[633], 9/2^+[624]) \otimes \pi^3(7/2^+[404], 7/2^-[523], 9/2^-[514])$$

configuration, while the level at 5417 keV is interpreted as its first rotational band member.

IV. TRANSITION STRENGTHS

The isomeric nature of the states in ^{174}Lu arises in principle from the fact that the depopulating transitions are K-forbidden. For a transition of multipole order, λ, the reduced hindrance factor per degree of K-forbiddenness, f_ν, with $\nu = \Delta K - \lambda$, is defined as $f_\nu = F^{1/\nu}$, where $F = T^\gamma_{1/2}/T^W_{1/2}$ and $T^\gamma_{1/2}$, and $T^W_{1/2}$ are the partial γ-ray and the Weisskopf estimate half-lives, respectively. The values deduced for transitions depopulating the isomers in ^{174}Lu are presented in Table I. The anomalously low values for the 427.1-keV ($\nu = 11$) and 267.4-keV ($\nu = 12$) transitions, depopulating the $K^\pi = 13^+$ isomer, were attributed in the earlier work to accidental mixing between the isomer and the 13^+ member of the $K^\pi = 0^+$ band [9]. A detailed analysis was presented there on both the effect of this mixing and of Coriolis mixing in the lower states from the $K^\pi = 0^+$ and 7^+ two-quasiparticle bands.

The observed value of $f_\nu = 79$ for the 299.2-keV $E1$ transition ($\nu = 4$), depopulating the $K^\pi = (26^-)$ isomer, is acceptable for a K-hindered decay. Although an additional (arbitrary) retardation factor of $\sim 10^3$ is sometimes incorporated in interpreting $E1$ transition strengths, both within ^{174}Lu (for example the $E1$ decay from the 13^+ isomer) and in nearby nuclei (e.g., in ^{174}Yb [7]), it does not seem necessary to include such a reduction here. The $K^\pi = (21^+)$ isomer decays via a K-allowed 328.1-keV ($E2$) transition with a strength of $2.5(3) \times 10^{-2}$ W.u. to the intrinsic (19^+) state at 3741 keV. In this case, the observed lifetime is a consequence of the rearrangement of several orbitals between the initial ($\nu^3\pi^3$) and final ($\nu^5\pi$) configurations (see Table II) that leads to a relatively slow $E2$ transition.

The limits on the reduced hindrances for the transitions from the 3741-keV state itself (Table I) are at the margin, particularly the $E2$ transition which has $f_\nu < 55$, but this is entirely consistent with the earlier conjecture that the intrinsic state is likely to be mixed with the 19^+ band level, thus enabling a faster transition, even with a very small admixture.

V. SUMMARY AND CONCLUSIONS

Multi-quasiparticle intrinsic states have been observed in the odd-odd nuclide ^{174}Lu from γ-ray spectroscopic studies with deep-inelastic and multinucleon transfer reactions. Four new isomers are identified, the highest being the 5850-keV state with a half-life of 242 ns. On the basis of multi-quasiparticle calculations, this isomer has been associated with a predicted $K^\pi = 26^-$ eight-quasiparticle state from a $\nu^5\pi^3$ configuration. Other isomers include the 194-ns 13^+ state, previously identified at 1856 keV, a 38-ns 14^- isomer at 2063 keV, and a 97 ns isomer at 4069 keV. Associated rotational bands for each of these long-lived states have also been identified, aiding in the configuration assignments. Other intrinsic states, which are not isomers within the present experimental limits, include (15^+), (16^+), and (19^+) levels at 2732, 2876, and 3741 keV. Configuration assignments are proposed for each of these, although some ambiguities remain in terms of calculated energies in this spin regime.

ACKNOWLEDGMENTS

The authors thank R. B. Turkentine for producing the targets, and S. J. Freeman and N. J. Hammond for assistance in the experiments. This work is supported by the US Department of Energy, Office of Science, Office of Nuclear Physics, under Contract No. DE-AC02-06CH11357 and Grant No. DE-FG02-94ER40848, the ANSTO program for Access to Major Research Facilities, Grant No. 02/03-H-05, and the Australian Research Council Discovery projects DP0343027 and DP0345844.

[1] P. M. Walker and G. D. Dracoulis, Nature (London) **399**, 35 (1999).
[2] R. Broda, M. A. Quader, P. J. Daly, R. V. F. Janssens, T. L. Khoo, W. C. Ma, and M. W. Drigert, Phys. Lett. **B251**, 245 (1990).
[3] R. Broda, C. T. Zhang, P. Kleinheinz, R. Menegazzo, K.-H. Maier, H. Grawe, M. Schramm, R. Schubart, M. Lach, and S. Hofmann, Phys. Rev. C **49**, R575 (1994).
[4] R. D'Alarcao *et al.*, Phys. Rev. C **59**, R1227 (1999).
[5] G. D. Dracoulis *et al.*, Phys. Lett. **B584**, 22 (2004).
[6] F. G. Kondev *et al.*, Eur. Phys. J. A **22**, 23 (2004).
[7] G. D. Dracoulis *et al.*, Phys. Rev. C **71**, 044326 (2005).
[8] G. D. Dracoulis *et al.*, Phys. Lett. **B635**, 200 (2006).
[9] G. D. Dracoulis *et al.*, Phys. Rev. Lett. **97**, 122501 (2006).
[10] R. Broda, J. Phys. G: Nucl. Part. Phys. **32**, R151 (2006).
[11] A. Bruder, S. Drissi, V. A. Ionescu, J. Kern, and J. P. Vorlet, Nucl. Phys. **A474**, 518 (1987).
[12] A. Bruder, J.-Cl. Dousse, S. Drissi, M. Gasser, V. A. Ionescu, J. Kern, B. Perny, M. Rast, and Ch. Rhéme, Nucl. Phys. **A467**, 1 (1987).
[13] S. Drissi, J. Kern, and E. Hagn, Nucl. Phys. **A512**, 413 (1990).
[14] J. Kern, J. B. Carlson, R. G. Lanier, L. G. Mann, and G. L. Struble, Z. Phys. A **296**, 195 (1980).
[15] J. Kern, A. Bruder, J.-Cl. Dousse, M. Gasser, V. A. Ionescu, R. Lanners, B. Perny, B. Piller, Ch. Rhéme, and B. Schaller, Phys. Lett. **B146**, 183 (1984).
[16] J.-Cl. Dousse, M. Gasser, J. Kern, V. A. Ionescu, B. Perny, and Ch. Rhéme, Helv. Phys. Acta **57**, 811 (1984).
[17] R. V. F. Janssens and F. S. Stephens, Nuclear Physics News **6**, 9 (1996).
[18] T. Kibédi, T. W. Burrows, M. B. Trzhaskovskaya, P. M. Davidson, and C. W. Nestor, Jr., Nucl. Instrum. Methods Phys. Res. A **589**, 202 (2008).
[19] S. Bayer, A. P. Byrne, and G. D. Dracoulis, Nucl. Phys. **A591**, 104 (1995).
[20] Jing-ye Zhang, A. J. Larabee, and L. L. Riedinger, J. Phys. G **13**, L75 (1987).
[21] P. Moller, J. R. Nix, W. D. Myers, and W. J. Swiatecki, At. Data Nucl. Data Tables **59**, 185 (1995).
[22] V. V. Shirley, Nucl. Data Sheets **75**, 377 (1995).
[23] M. S. Basunia, Nucl. Data Sheets **102**, 719 (2004).
[24] K. Jain, O. Burglin, G. D. Dracoulis, B. Fabricius, P. M. Walker, and N. Rowley, Nucl. Phys. **A591**, 61 (1995).
[25] F. G. Kondev, Ph.D. thesis, Australian National University, 1996 (unpublished).
[26] R. O. Hughes, G. J. Lane, G. D. Dracoulis, T. Kibédi, P. Nieminen, and H. Watanabe, Phys. Rev. C **77**, 044309 (2008).
[27] S. Cwiok, J. Dudek, W. Nazarewicz, J. Skalski, and T. Werner, Comput. Phys. Commun. **46**, 379 (1987).
[28] G. D. Dracoulis, F. G. Kondev, and P. M. Walker, Phys. Lett. **B419**, 7 (1998).
[29] P. M. Walker, G. D. Dracoulis, A. P. Byrne, B. Fabricius, T. Kibédi, A. E. Stuchbery, and N. Rowley, Nucl. Phys. **A568**, 397 (1994).
[30] F. G. Kondev, Nucl. Data Sheets **98**, 801 (2003).